Hindawi
International Journal of Photoenergy
Volume 2021, Article ID 7176506, 9 pages
https://doi.org/10.1155/2021/7176506

Research Article

A Comparative Performance Analysis between Serpentine-Flow Solar Water Heater and Photovoltaic Thermal Collector under Malaysian Climate Conditions

M. S. Hossain,[1] **Laveet Kumar**,[2] **and Afroza Nahar**[3]

[1]*College of Environmental Science and Engineering, Peking University, Beijing 100871, China*
[2]*Department of Mechanical Engineering, Mehran University of Engineering and Technology, Jamshoro, 76090 Sindh, Pakistan*
[3]*Department of Computer Science, Faculty of Science and Technology, American International University–Bangladesh, Dhaka 1229, Bangladesh*

Correspondence should be addressed to Afroza Nahar; afroza@aiub.edu

Received 15 June 2021; Accepted 30 August 2021; Published 16 September 2021

Academic Editor: Mohammad Alhuyi Nazari

Solar energy has increasingly been employed for domestic and industrial water heating. Both conventional solar water heater (SWH) and photovoltaic thermal (PVT) systems suffer from the drawback of poor energy conversion efficiency. In this article, a unique parallel serpentine-flow thermal collector has been designed and developed that has been employed as an isolated SWH and also integrated with a 32-cell monocrystalline photovoltaic (PV) module. Simulation models of both SWH and PVT systems have been built in TRNSYS to study their thermal performance numerically. Thereafter, outdoor experimental investigations have been conducted under the composite climates of Malaysia. Experimental results show very good agreement with the simulation outcomes with disparity less than 2%. At the optimum flow rate, the maximum thermal efficiencies of SWH and PVT are 82.5% and 74.62%, respectively. Superior water outlet temperature was obtained with SWH. Although SWH exhibits superior thermal performance, PVT's additional electrical output might make it preferable for several applications.

1. Introduction

Global energy consumption is exponentially increasing with increased economic activities of the human civilization. According to the World Resources Institute [1], the level of economic activities performs a substantial role in the emission of greenhouse gases (GHG). And the intensity of CO_2 emission of a country is totally dependent on the energy supply system it has adopted, whether coal and oil based or renewable based [2]. Renewable energy sources such as solar, wind, biogas, biomass, hydropower, and geothermal provide low carbon alternatives of energy sources. However, renewable energy accounted for only 1.6% of global energy demand in 2012 and is expected to increase to 2.2% in 2035 [3]. Among the other renewables, solar energy has benefits like wider access and greater predictability; hence, application of solar energy is expanding day-by-day, especially in water and space heating, desalination, and power generation [4].

Several machineries have been developed to exploit solar energy in the form of heat, electricity, and both. Among the solar technologies, the solar water heating (SWH) system is a well-developed platform in exploiting solar energy, while the photovoltaic thermal (PVT) system is still under development. There are many types of solar thermal collectors for SWH application, but most of them are fixed or centralized. The fixed type includes the flat plate collector (FPC), evacuated tube collectors (ETC), composite parabolic collectors (CPC), cylindrical trough collectors (CTC), and heliostat field collectors (HFC) [5–7]. Thermal efficiency (η_{th}) of an FPC system depends on the absorber or thermal collector design. Many thermal collector configurations have been reported in the literature, e.g., oscillating flow (η_{th} 60%), spiral flow (η_{th} 70%), serpentine flow (η_{th} 48%), parallel serpentine

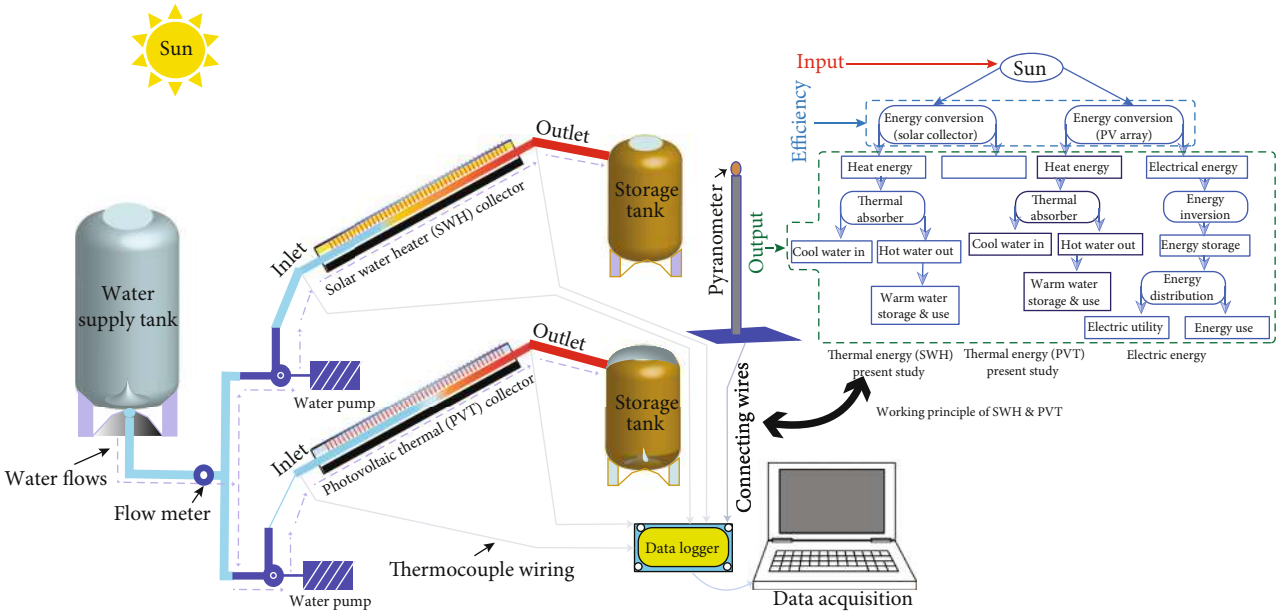

Figure 1: Schematic of SWH and PVT systems.

flow (η_{th} 70%), orbital flow (η_{th} 62%), modified serpentine or parallel (η_{th} 68%), and V-trough (η_{th} 70%) [8].

Jiandong et al. [9] numerically investigated the thermal efficiency of an FPC and observed that as the collection tube length or diameter decreases, efficiency of the collector increases. Belkassmi et al. [10] numerically studied the impact of using nanofluids on the operation of an FPC where copper/water, copper oxide/water, and alumina/water nanofluids have been used. Authors reported average gains in thermal efficiency of 4.44%, 4.27%, and 4.21% with copper/water, copper oxide/water, and alumina/water, respectively. Computational models for solar thermal systems developed in recent years eradicated the need for onsite experiments to a good extent [11]. In this regard, TRNSYS software is reportedly apposite for the SWH and PVT systems to assess their thermal and overall performances [12, 13].

Both SWH and PVT are commonly used for domestic hot water [14], and the thermal collector part (or absorber) of these collectors is usually made from a high thermal conductivity metal plate attached with channels for heat transfer fluid (HTF) flow. The surface is painted or coated to increase the absorption of radiant energy and sometimes to limit radiation [15]. The protected box provides structure and fixation and reduces heat loss on the back or side of the manifold. The covering foil, the so-called liner, allows sunlight to enter the absorber and protects the space in the absorber by preventing the passage of cold air. In any case, the glass will reflect some sunlight that has not reached the absorber [16]. PVT manifolds can be designed for temperatures as high as 200°C. Therefore, its absorber is usually made of copper, steel, or aluminum. On the other hand, the collector box can be made of plastic, metal, or wood, and a glass cover must be attached to prevent heat from escaping, and the heat collector itself can be dust-proof. The collector itself is shielded from dust and dirt, creepy crawlies, or sticky substances [8, 17].

Despite the use of insulating material in the collector box, a certain amount of heat loss is inevitable due to the temperature gradient between the glass cover, absorber, and ambient air. These convection losses are caused by the critical point—the scattering effect between the glass cover and the absorption plate. In contrast, radiation loss is caused by the heat exchange between the absorbent and the environment [18]. The absorption plate covering the entire area of the collector hole has three functions: (i) absorb as much radiation as possible, (ii) release heat from the working medium with the slightest temperature difference, and (iii) release the measured baseline heat into the environment [19]. Other parts of the collector, such as storage tanks, can be connected to the water inlet and outlet flows.

Electrical efficiency of PV cells deteriorates with increasing cell temperature, and if this unwanted heat can be efficiently extracted from the cell, it might be utilized for low- to medium-temperature thermal applications [17, 20, 21]. On the one hand, air or water cooling for flat plate or concentrator collectors employed for standalone or building-integrated PV realizes increase in electrical efficiency up to 12–14% [22]; on the other hand, effective utilization of the waste heat extracted from the panels reportedly improves the thermal performance by a higher margin [23–26]. A numerical model predicts that using high thermal conductivity nanofluids can extract heat from the modules more efficaciously than air and water [27]. Hence, for better thermal and electrical performance, nanoparticles that enhance the heat transfer rate can be doped into cooling water.

From the literature, it can be observed that the SWH and the PVT collector performance depends on the absorber channel design. However, the primary heat gain difference between the two collectors depends on main plate materials (glazed or unglazed). The present study introduces a newly developed single serpentine-flow thermal absorber design

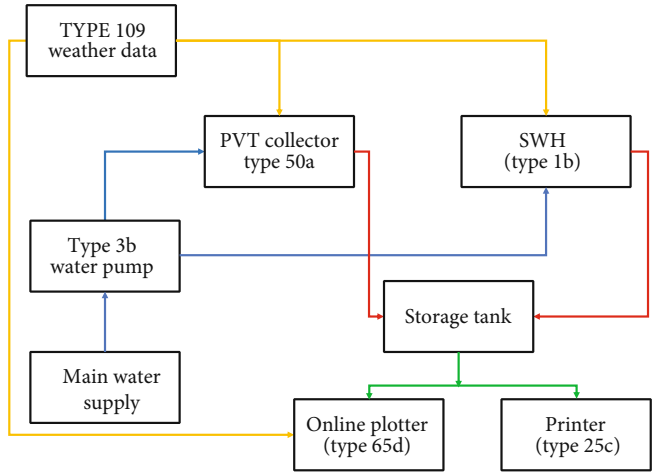

Figure 2: Block diagram of TRNSYS model.

and tests it in both systems, i.e., PVT and FPC, simultaneously to achieve the collector performance. Although the performance assessment of serpentine-flow thermal absorber-based PVT collectors has been investigated experimentally in the earlier study by the same group of authors, the focus of that study was limited only to PVT-based systems. In the present research, dynamic simulation models of PVT and FPC have been compared. In addition to developing dynamic simulation models of SWH and PVT systems in TRNSYS, the collector's thermal performance is based on experimental field studies under typical conditions in Malaysia. The article's structure constitutes the following sections: modelling and simulation, experimental analysis, results and discussion, and conclusion. Finally, a comparative study is conducted to evaluate the thermal performance between SWH and PVT collectors to realize the overall merit of these systems.

2. Research Methodology

2.1. Modeling and Simulation in TRNSYS. Figure 1 shows an overall concept of the SWH and PVT systems and their specific working methods. In this study, the SWH and PVT collectors are serpentine-flow-based flat plate collectors. The SWH system collects solar heat and supplies it directly into the inlet water. On the other hand, the PVT system is combined with the PV module and FPC, wherein the waste heat from the PV module is transferred to the thermal collector that warms up the water flowing through the attached channels.

This analysis is aimed primarily at performing a dynamic simulation of two systems under Malaysian climatic conditions. The following assumptions are considered in the TRNSYS modelling and simulation:

(i) The system is assumed as equilibrium

(ii) Energy losses are neglected in the connected piping and valves

(iii) Thermal properties remain constant

A block diagram of a TRNSYS model is illustrated in Figure 2. The comparative simulation of the solar hot water system based on serpentine SWH and PVT with TRNSYS is shown in Figures 3(a) and 3(b), respectively. The solid lines illustrate the various paths for water, and the dotted lines represent all other necessary joints. The Type 109-TMY2 is used to read weather data and provide the weather information to the model. The TMY2 weather file with data for Kaula Lumpur, Malaysia, used for the current analysis includes solar radiation and meteorological information for a given location which is important to predict the performance. The main components of the TRNSYS model are solar collectors, storage tank, pump, and unit control which are presented in detail as follows:

(i) Weather data component is Type 109, which reads the typical TMY2 format weather data file

(ii) Solar flat plate collector (SWH) is Type 1b which converts the irradiance into the internal energy of the working fluid

(iii) The photovoltaic thermal (PVT) collector is Type 50a which converts the irradiance energy into the working fluid's electrical and internal energy

(iv) Water pump is Type 3b

(v) Type 65d are online plotters

2.2. Experimental Investigation. The conceptual schematic of the experimental set-up comprising SWH and PVT systems is shown in Figure 1. The outdoor experimental set-up consists of a flat plate collector (FPC) with serpentine-flow channel and a photovoltaic thermal (PVT) collector with the same channel configuration. A water pump maintains the flow through the circuit and carries heat to the application end. This solar water heater has two different water tanks: one for cold water or regular water supply and the

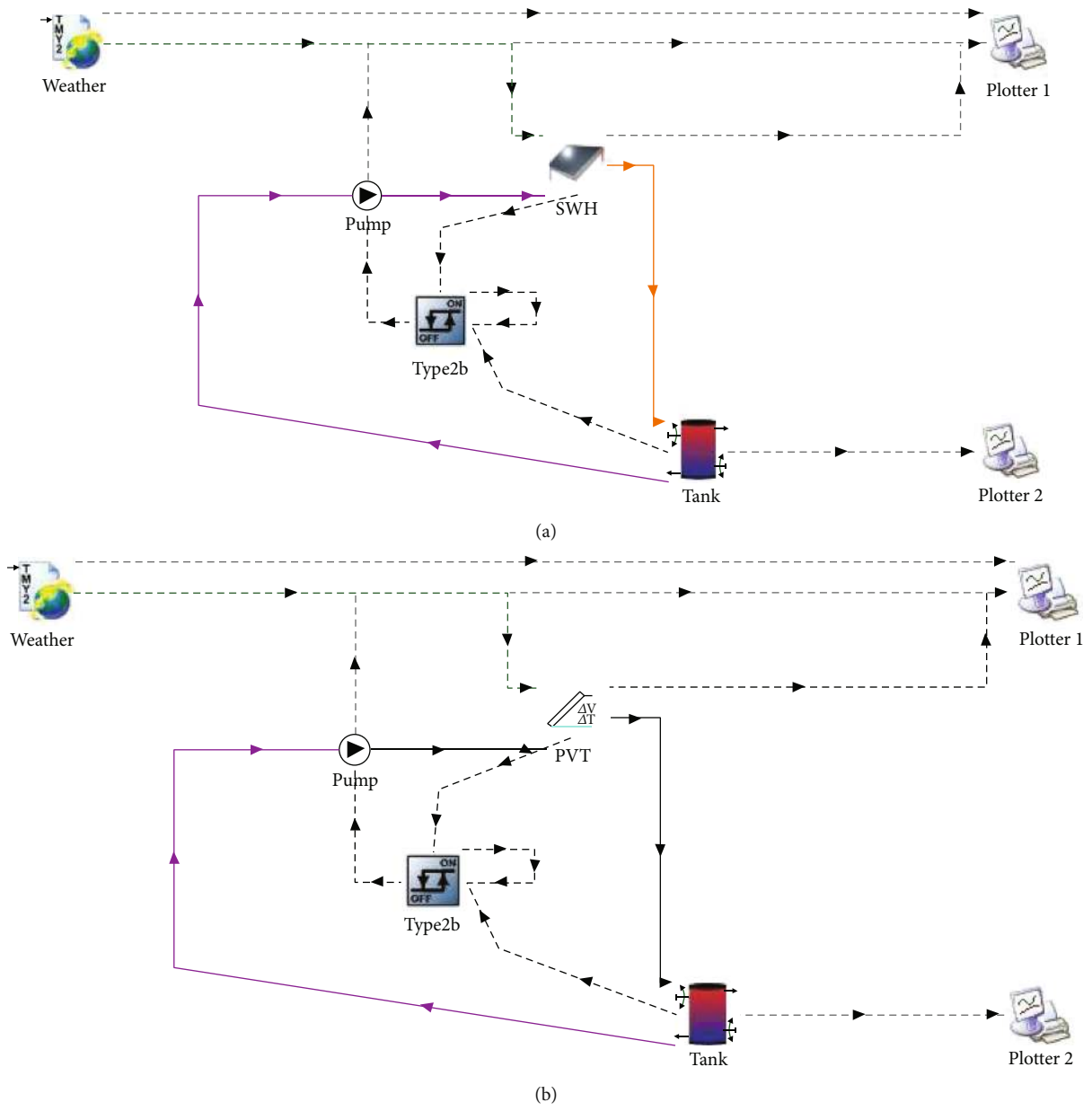

Figure 3: TRNSYS model for (a) SWH and (b) PVT systems.

other for storing hot water. There are several controller valves in the water tank to help with water transfer. The individual SWH and PVT collectors along with flow channel design and the monocrystalline Si PV module are illustrated in Figure 4. For instrumentation, K-type thermocouples are used to measure temperatures at different points, a flow meter is connected to measure the flow between the cold-water tank and the pump, and a silicon pyranometer is used to measure the solar irradiance. Real-time data have been recorded uninterruptedly in a digital data logger.

Copper tubes have been used in thermal collector fabrication because of their excellent thermal conductivity [28]. Due to the serpentine design and the number of loops in the channel, water will take a longer time to reach the exit that will allow more thermal energy to be absorbed and transported [29]. Moreover, this configuration ensures coverage of the most of the collector area that helps to harvest more waste heat.

2.3. Mathematical Framework for Thermal Performance Analysis. Conventional energy analysis consists of carrying out energy balances based on the first law of thermodynamics and determining energy efficiencies. The energy balance equation for all the systems under control volume in the equilibrium state is the following equations [12, 30, 31]:

$$\sum \dot{E}_{\text{in}} = \sum \dot{E}_{\text{out}} + \sum \dot{E}_{\text{loss}}, \tag{1}$$

or

$$\dot{E}_{\text{sun}} + \dot{E}_{\text{mass,in}} = \dot{E}_{\text{mass,out}} + \dot{E}_{\text{electrical}} + \dot{E}_{\text{loss}}, \tag{2}$$

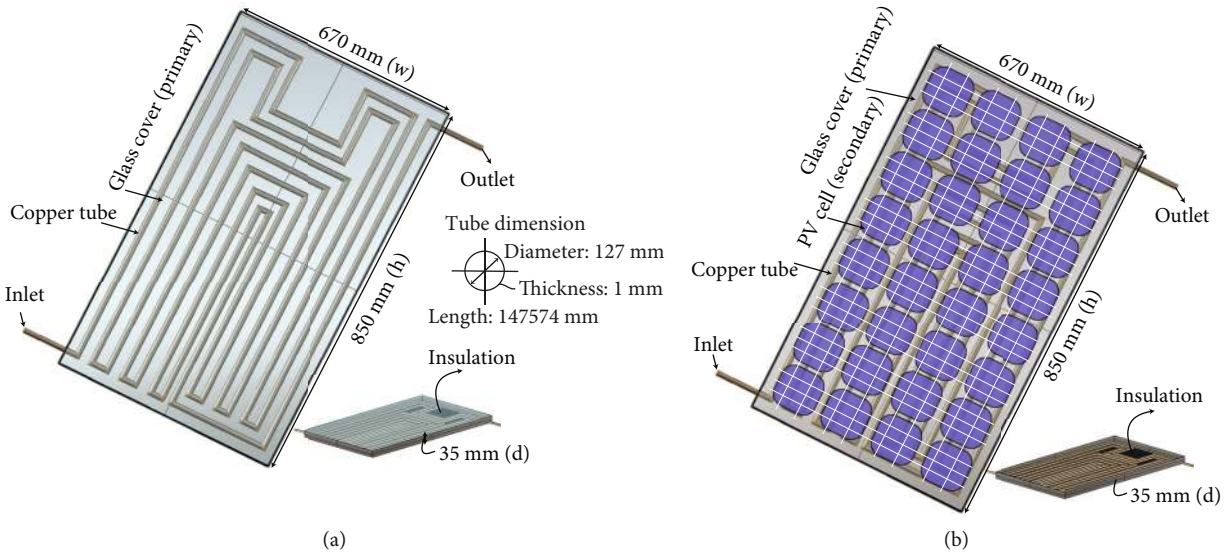

Figure 4: Fabricated model for (a) SWH and (b) PVT systems.

where $\dot{E}_{in}$, $\dot{E}_{out}$, and $\dot{E}_{loss}$ are the energy input, output, and loss, respectively. $\dot{E}_{electrical}$ is the amount of energy converted into electricity. $\dot{E}_{sun}$ is the solar energy and $\dot{E}_{mass,in}$ and $\dot{E}_{mass,out}$ are, respectively, the enthalpies of the inlet and outlet waters reaching the surface of both collectors, i.e., SWH and PVT, which can be calculated by

$$\dot{E}_{sun(SWH)} = \tau\alpha A_{SWH} I_{rad}, \quad (3)$$

$$\dot{E}_{sun(PVT)} = \tau\alpha A_{PVT} I_{rad}, \quad (4)$$

where τ and α are transmittance and absorptance coefficients of SWH and PVT, respectively. However, the collector coefficients may differ due to various materials. A is the area of the collector (m^2) and I_{rad} is the irradiation (W/m^2).

Under the above condition, the useful heat (energy) gain and thermal energy efficiency can be calculated as equation (5):

Collector heat gain:

$$\dot{E}_{gain} = \dot{m} C_p (T_{water,out} - T_{water,in}), \quad (5)$$

where $\dot{E}_{gain}$ is the collector heat gain, $\dot{m}$ is the mass flow rate of fluid (kg/s), and C_p is the specific heat at constant pressure (J/kg K). However, the water temperature (°C) difference between outlet and inlet can be represented by $T_{water,in}$ and $T_{water,out}$, respectively.

Efficiency of a collector is expressed by its thermal efficiency ($\eta_{Thermal}$), which is usually the ratio between the available heat gain of the system and the solar radiation incident on the gap of the collector over a period of time. Thermal energy efficiency can be calculated by using a traditional

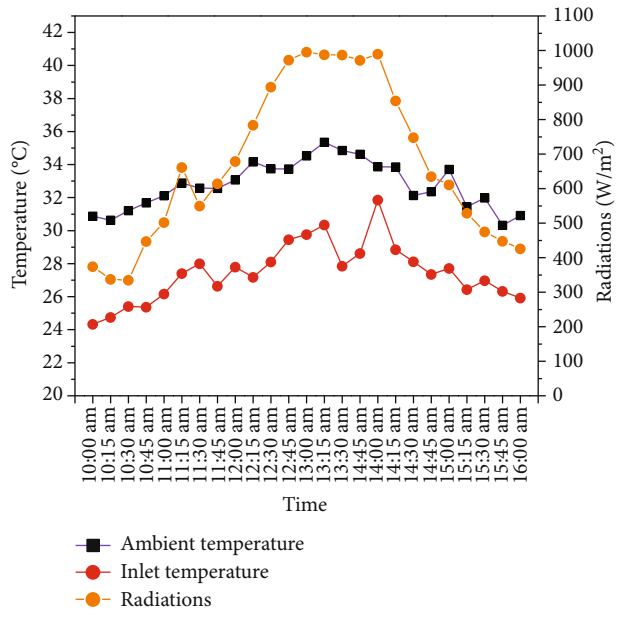

Figure 5: Water inlet temperature and surrounding weather conditions.

equation:

$$\eta_{Thermal} = \frac{\dot{E}_{gain}}{\dot{E}_{sun}}, \quad (6)$$

where $\eta_{Thermal}$ is the collector thermal efficiency. The SWH and PVT collector thermal efficiency is calculated by using equations (3), (4), and (5).

The solar energy absorbed by the PV modules is turned into electric and thermal energy, while the thermal energy is wasted through convection, conduction, and radiation.

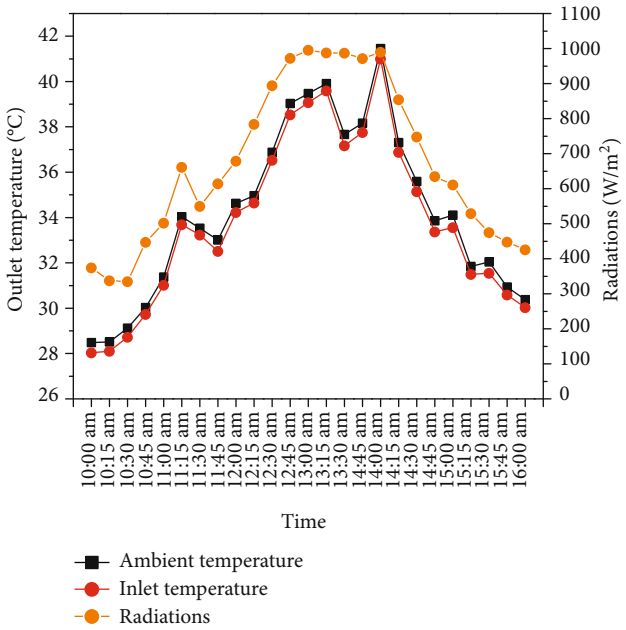

Figure 6: Simulated and experimental outlet temperatures for SWH system.

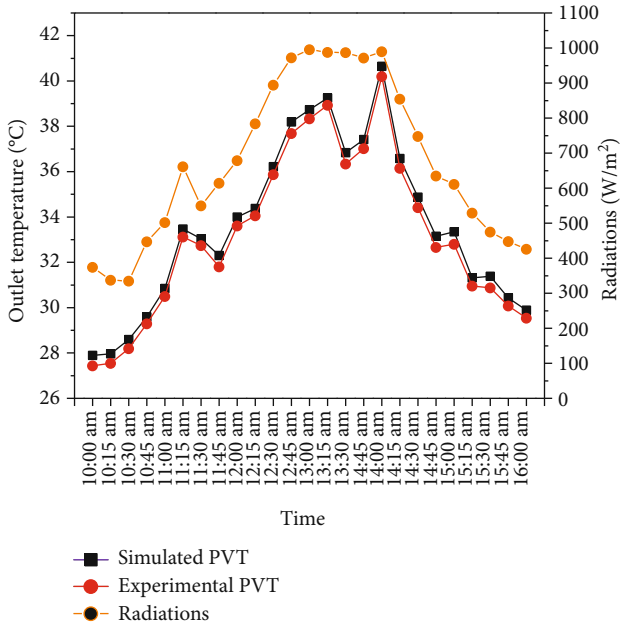

Figure 7: Simulated and experimental outlet temperatures for PVT system.

2.4. Error Analysis. An error analysis has been performed to check the relevance of the proposed TRNSYS model. The root mean square error (RMSE) is statistical data used to measure the degree of consistency between a simulated model and experimental physical results, which establishes character and allows for broader application of the model. In this analysis, RMSE is calculated using the following

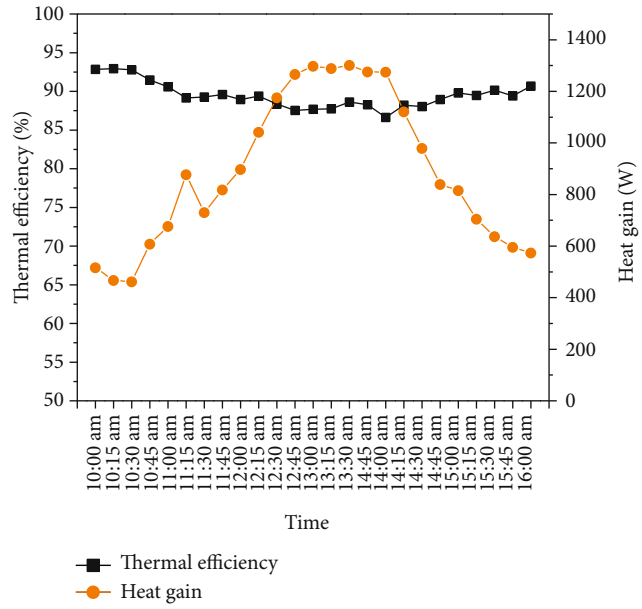

Figure 8: Thermal analysis of SWH system.

equation [32]:

$$\mathrm{RMSE} = \sqrt{\frac{\sum\left[100 \times \left(T_{\mathrm{Exp},n} - T_{\mathrm{Sim},n}\right)/T_{\mathrm{Exp},n}\right]^2}{N_{\mathrm{Exp}}}}, \quad (7)$$

where $T_{\mathrm{Exp},n}$ and $T_{\mathrm{Sim},n}$ are the experimental and simulated results at n, respectively, and N_{Exp} is the number of experimental points executed.

Comparison of the experimental and simulated results revealed very good agreement with the maximum standard error of less than 2%. Such a low margin of RMSE provides the acceptance of simulated results [32].

3. Results and Discussion

This section presents a comparative performance assessment of serpentine-flow SWH and PVT systems with conforming explanations wherever necessary. The outcomes have been explained in three parts: first, onsite weather parameters and its effect on water temperature; secondly, effect of solar irradiance on system performance; and thirdly, a performance comparison with previous reported systems.

3.1. Hourly Weather Data Variations and Outlet Temperature. The TRNSYS model central input data come from global weather data and the experimental data collected by different parameters, such as irradiance, the surrounding (ambient) temperature, and collector inlet water temperature. The irradiance intensity is available in Malaysia. It is recorded that the average irradiance range is 4500 kWh per square meter, which can be a perfect place for large-scale solar power plant installation. It is expected that if the amount of irradiance it gets every day is about 4.5 to 8 hours, it will be good enough to produce high solar power generation; however, the solar-based application is

still minor than expected in Malaysia. Figure 5 shows an hourly variation (8 hours) of SWH and PVT collector inlet water temperature. The inlet temperature is measured at the water flow rate of 0.034 kg/s.

Figures 6 and 7 show the simulated and experimental variations of outlet water temperature under varying solar radiations. Figures 6 and 7 show both simulated and experimental trends of the outlet temperature as a function of irradiation at 0.5 LPM for SWH and PVT. It is quite apparent that simulated results agree well with the experimental outcome in all cases.

In this part, the irradiance and surrounding temperature data are entirely understood, which varies with time. There can be three practical situations in irradiance and surrounding temperature data. At 10 am, the surrounding temperature and irradiance data are recorded at 380 W/m^2, 31°C, then rise to a peak irradiance at 989 W/m^2, 33°C, and the last stage irradiance data is at 430 W/m^2 at 4 pm where the surrounding temperature was 31°C. However, the weather behaviour cannot be controlled.

Although there are several unusual sharp declines in the irradiance curve, irradiance is at its peak from 1:00 to 2:00 pm. However, variation in the surrounding temperature throughout the day does not follow the same trend as in the case of irradiation; instead, it remains almost constant all along the day with slight variation. Figure 6 also gives a shred of evidence that the temperature rise in water is directly proportional to the hourly variation in irradiance with the increasing trend in the morning, the highest increase at noon, and then a decreasing trend. The maximum inlet temperature is at 32°C at 2 pm and falls at 25°C at 4 pm.

Figure 7 represents the PVT simulation and experimental results in the hourly variation of irradiance and outlet water temperatures at the typical water flow rate of 0.034 kg/s. It is observed that the outlet water temperature is 40°C (maximum rise) at 2 pm, whereas the irradiance was 989 W/m^2 and the surrounding temperature was 33°C. Figure 6 also points to the same statement that the temperature rise in water is directly proportional to the hourly variation in irradiance with the increasing trend in the morning, the highest increase in the noon, and then decreasing trend. The maximum water (inlet and outlet) temperature difference was 9°C when the irradiance was picked. However, the outlet water temperature difference between simulated and experimental results is negligible. It is justified that the TRNSYS model outcomes and experiment performance are in the same trend.

3.2. Effect of Solar Irradiances on the Thermal Performance at an Optimum Mass Flow Rate. Performance solar collector systems mainly depend on the intensity of solar irradiance. Calculating the thermal performance of those systems focuses on collector heat gain and irradiance (equation (5)). In this section, thermal efficiency and heat gain of the collectors have been displayed as a daytime function which portrays the variation solar irradiance level of that day.

Figures 8 and 9 show the thermal performance of SHW and PVT collectors in terms of outlet water temperature,

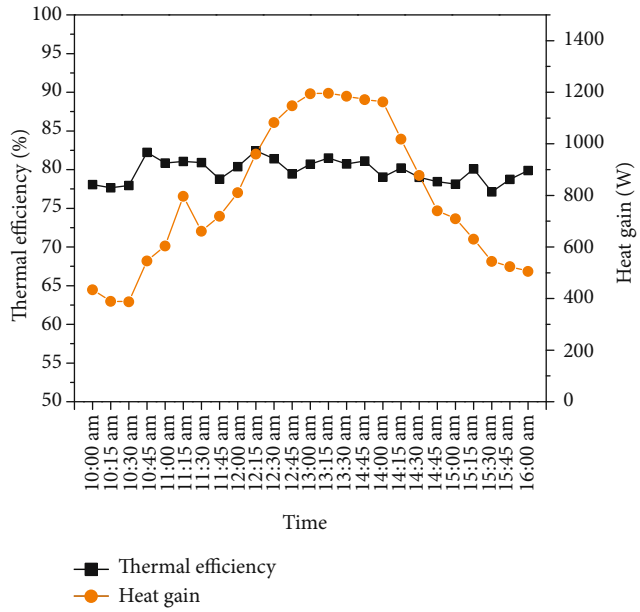

Figure 9: Thermal analysis of PVT system.

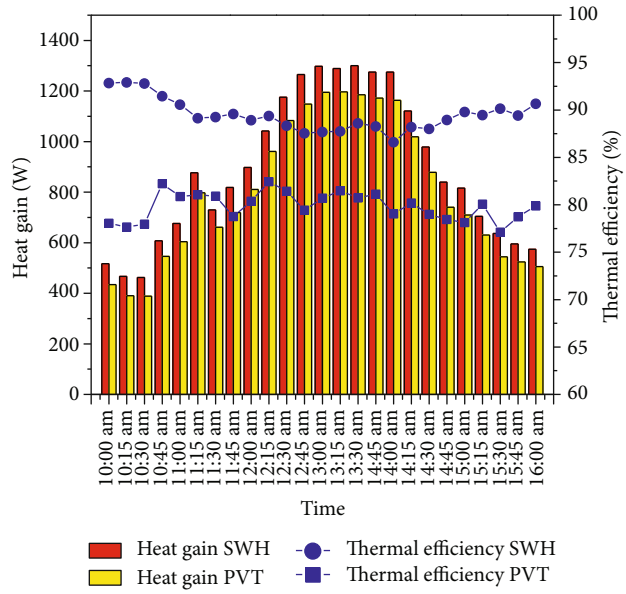

Figure 10: Comparative performance analysis between SWH and PVT.

heat gain, and efficiency. The maximum heat gain in the SWH system is 1300 W at 1.30 pm. Whereas, the PVT system got 1200 W at 1.15 pm. The highest thermal efficiency obtained for both systems is 93% at 10.15 am and 83% at 10.45 a.m. At the same time, the average thermal efficiency is 82.5% and 74.62%, respectively.

It can be observed that the heat gain for each system's trend follows a bell-shaped curve. The trend is similar, but PVT values are lower than the SWH system. However, the thermal efficiency distribution values are not the same nor symmetrical because of PVT materials. Another significant point can be noticed in both systems' heat gain and

Table 1: Comparative results of performance of present and previous studies.

System		Study scope (simulation/experimental)	Thermal efficiency (%)	Reference
PVT-nanofluids		Simulation	70-75	[5]
ICS-SWH		Experimental	66.7	[33]
PVT and PVT glazed		Experimental	66 and 50	[34, 35]
Self-cleaning PVT with PCM		Experimental	77.6	[36]
PVT	Sheet and tube	Simulation and experimental	52-66	[37]
	Box channels	Simulation and experimental	45-76	
	Roll bond	Simulation and experimental	49.3-79	
SWH and PVT		Simulation and experimental	82.5 and 74.62	Present study

efficiency difference, which can give a clear justification. In a PVT system, the thermal energy is removed; thus, the electricity production can be increased.

3.3. Comparative Performance Analysis between SWH and PVT Systems. In this section, a comparative performance has evaluated the SWH and PVT systems to make a relative ranking among the systems possible. Figure 10 shows the thermal performance of the SWH and PVT systems. The heat gain and thermal efficiency of the SWH system perform better than those of the PVT system because at the PVT collector, the main plate is covered with a PV module. So, most of the thermal energy is absorbed by cells, and then, heat flows to the absorber tube. The result shows that PVT's maximum thermal efficiency and that of SWH are 74.62% and 82.5% at the optimum flow rate, respectively. The results obtained in this study are comparable to the results of other investigators in the literature.

3.4. Performance Comparison with Previous Studies. The overall thermal comparative results of performance of the present study and a previous study are shown in Table 1. It is investigated that the present SWH thermal efficiency has significant achievement with previous study results. On the other hand, only PVT thermal efficiency is slightly lower than box channels by 1.38% and roll bond by 4.38% due to the different materials, mass flow rates, and experimental location. To evaluate the performance of the absorber system, a single SWH system can be a more suitable option. In the literature, there are seven different absorber systems and their thermal performance [8]. The proposed unique parallel serpentine-flow absorber significantly improves from the previous study due to its materials and techniques.

4. Conclusions

This study investigates and analyzes the collector performance of newly developed SHW and PVT systems with a serpentine-flow thermal collector under typical Malaysian weather conditions. Besides that, a comparative performance has been made in the following manner: firstly, the SHW and PVT systems; secondly, the analytical and energetic performance.

The proposed active system and hourly data were collected for this research. It is clear from the analysis of the results that the collector's thermal performance depends on radiant solar energy, water temperature difference, and thermal conductivity. However, the thermal efficiency-related trends were explained with thermodynamic laws.

The result shows that the maximum thermal efficiencies of PVT and SWH are 74.62% and 82.5% at the optimum flow rate of 0.034 kg/s, respectively. Also, the comparative study shows that the outlet water temperature was higher in SWH. Comparison of the experimental and simulated results revealed a perfect agreement with the maximum standard error of less than 2%.

Data Availability

Data can be provided on request by contacting the corresponding author.

Conflicts of Interest

The authors declare that they have no conflicts of interest.

Acknowledgments

This work is the manuscript of a dissertation submitted at the University of Malaya, Malaysia.

References

[1] WRI, *5 big findings from the IPCC's new climate report*, World Resources Institute, 2021.

[2] M. Ghalandari, H. Forootan Fard, A. Komeili Birjandi, and I. Mahariq, "Energy-related carbon dioxide emission forecasting of four European countries by employing data-driven methods," *Journal of Thermal Analysis and Calorimetry*, vol. 144, no. 5, article 10400, pp. 1999–2008, 2021.

[3] A. Maleki, A. Haghighi, M. el Haj Assad, I. Mahariq, and M. Alhuyi Nazari, "A review on the approaches employed for cooling PV cells," *Solar Energy*, vol. 209, pp. 170–185, 2020.

[4] IEO, *International energy outlook 2016*, U.S. Energy Information Administration, 2016.

[5] B. Darbari and S. Rashidi, "Thermal efficiency of flat plate thermosyphon solar water heater with nanofluids," *Journal of the Taiwan Institute of Chemical Engineers*, pp. 1–12, 2021.

[6] A. Ahmadi, M. A. Ehyaei, A. Doustgani et al., "Recent progress in thermal and optical enhancement of low temperature solar collector," *Energy Systems*, 2021.

[7] L. Kumar, M. Hasanuzzaman, and N. A. Rahim, "Global advancement of solar thermal energy technologies for industrial process heat and its future prospects: a review," *Energy Conversion and Management*, vol. 195, pp. 885–908, 2019.

[8] I. Adnan, M. Y. Othman, M. H. Ruslan et al., "Performance of photovoltaic thermal collector (PVT) with different absorbers design. ISSN: 1790-5079," *WSEAS Transactions on Environment and Development*, vol. 5, no. 3, pp. 321–330, 2009.

[9] Z. Jiandong, T. Hanzhong, and C. Susu, "Numerical simulation for structural parameters of flat-plate solar collector," *Solar Energy*, vol. 117, pp. 192–202, 2015.

[10] Y. Belkassmi, K. Gueraoui, L. el maimouni, N. Hassanain, and O. Tata, "Numerical investigation and optimization of a flat plate solar collector operating with Cu/CuO/Al_2O_3–Water nanofluids," *Transactions of Tianjin University*, vol. 27, no. 1, pp. 64–76, 2021.

[11] S. M. Mortazavinejad and M. Mozafarifard, "Numerical investigation of two-dimensional heat transfer of an absorbing plate of a flat-plate solar collector using dual-reciprocity method based on boundary element," *Solar Energy*, vol. 191, pp. 332–340, 2019.

[12] L. Kumar, M. Hasanuzzaman, N. A. Rahim, and M. M. Islam, "Modeling, simulation and outdoor experimental performance analysis of a solar- assisted process heating system for industrial process heat," *Renewable Energy*, vol. 164, pp. 656–673, 2021.

[13] L. Kumar, M. Hasanuzzaman, and N. Rahim, "Real-time experimental performance assessment of a photovoltaic thermal system cascaded with flat plate and heat pipe evacuated tube collector," *Journal of Solar Energy Engineering*, vol. 144, no. 1, article 011004, 2022.

[14] M. Jahangiri, E. T. Akinlabi, and S. M. Sichilalu, "Assessment and modeling of household-scale solar water heater application in Zambia: technical, environmental, and energy analysis," *International Journal of Photoenergy*, vol. 2021, Article ID 6630338, 13 pages, 2021.

[15] S. Dubey and G. N. Tiwari, "Thermal modeling of a combined system of photovoltaic thermal (PV/T) solar water heater," *Solar Energy*, vol. 82, no. 7, pp. 602–612, 2008.

[16] I. Grigorios, *Flat-plate solar collectors for water heating with improved heat transfer for application in climatic conditions of the Mediterranean region, Durham E-Theses*, School of Engineering and Computing Science, Durham University, 2009.

[17] K. K. Chong, K. G. Chay, and K. H. Chin, "Study of a solar water heater using stationary V-trough collector," *Renewable Energy*, vol. 39, no. 1, pp. 207–215, 2012.

[18] A. S. Joshi, I. Dincer, and B. V. Reddy, "Performance analysis of photovoltaic systems: a review," *Renewable and Sustainable Energy Reviews*, vol. 13, no. 8, pp. 1884–1897, 2009.

[19] K. S. Ong, *Solar Water Heaters Engineering and Applications*, University of Malaya Press, 1994.

[20] A. Jaaz, H. Hasan, K. Sopian, A. Kadhum, T. Gaaz, and A. al-Amiery, "Outdoor performance analysis of a photovoltaic thermal (PVT) collector with jet impingement and compound parabolic concentrator (CPC)," *Materials*, vol. 10, no. 8, p. 888, 2017.

[21] M. M. Islam, M. Hasanuzzaman, N. A. Rahim, A. K. Pandey, M. Rawa, and L. Kumar, "Real time experimental performance investigation of a NePCM based photovoltaic thermal system: an energetic and exergetic approach," *Renewable Energy*, vol. 172, pp. 71–87, 2021.

[22] H. G. Teo, P. S. Lee, and M. N. A. Hawlader, "An active cooling system for photovoltaic modules," *Applied Energy*, vol. 90, no. 1, pp. 309–315, 2012.

[23] A. Makki, S. Omer, and H. Sabir, "Advancements in hybrid photovoltaic systems for enhanced solar cells performance," *Renewable and Sustainable Energy Reviews*, vol. 41, pp. 658–684, 2015.

[24] P. Lianos, "Review of recent trends in photoelectrocatalytic conversion of solar energy to electricity and hydrogen," *Applied Catalysis B: Environmental*, vol. 210, pp. 235–254, 2017.

[25] V. V. Tyagi, S. C. Kaushik, and S. K. Tyagi, "Advancement in solar photovoltaic/thermal (PV/T) hybrid collector technology," *Renewable and Sustainable Energy Reviews*, vol. 16, no. 3, pp. 1383–1398, 2012.

[26] A. K. Pandey, M. S. Hossain, V. V. Tyagi, N. Abd Rahim, J. A. L. Selvaraj, and A. Sari, "Novel approaches and recent developments on potential applications of phase change materials in solar energy," *Renewable and Sustainable Energy Reviews*, vol. 82, pp. 281–323, 2018.

[27] A. Maleki, A. Haghighi, and I. Mahariq, "Machine learning-based approaches for modeling thermophysical properties of hybrid nanofluids: a comprehensive review," *Journal of Molecular Liquids*, vol. 322, article 114843, 2021.

[28] T. E. Toolbox, "Thermal conductivity of common materials and gases," 2021, https://www.engineeringtoolbox.com/thermal-conductivity-d_429.html/.

[29] M. S. Hossain, A. K. Pandey, M. A. Tunio, J. Selvaraj, K. E. Hoque, and N. A. Rahim, "Thermal and economic analysis of low-cost modified flat-plate solar water heater with parallel two-side serpentine flow," *Journal of Thermal Analysis and Calorimetry*, vol. 123, no. 1, pp. 793–806, 2016.

[30] M. el Haj Assad, A. Khosravi, M. AlShabi, B. Khuwaileh, and A. K. Hamid, "Energy and cost analysis of processing flat plate solar collectors," *Energy Engineering: Journal of the Association of Energy Engineering*, vol. 118, no. 3, pp. 447–458, 2021.

[31] M. A. Ehyaei, A. Ahmadi, M. E. H. Assad, A. A. Hachicha, and Z. Said, "Energy, exergy and economic analyses for the selection of working fluid and metal oxide nanofluids in a parabolic trough collector," *Solar Energy*, vol. 187, pp. 175–184, 2019.

[32] T. Ma, M. Li, and A. Kazemian, "Photovoltaic thermal module and solar thermal collector connected in series to produce electricity and high-grade heat simultaneously," *Applied Energy*, vol. 261, article 114380, 2020.

[33] R. Panahi, M. H. Khanjanpour, A. A. Javadi, M. Akrami, M. Rahnama, and M. Ameri, "Analysis of the thermal efficiency of a compound parabolic integrated collector storage solar water heater in Kerman, Iran," *Sustainable Energy Technologies and Assessments*, vol. 36, article 100564, 2019.

[34] J.-H. Kim and J.-T. Kim, "The experimental performance of an unglazed PVT collector with two different absorber types," *International Journal of Photoenergy*, vol. 2012, Article ID 312168, 6 pages, 2012.

[35] J.-H. Kim and J.-T. Kim, "Comparison of electrical and thermal performances of glazed and unglazed PVT collectors," *International Journal of Photoenergy*, vol. 2012, Article ID 957847, 7 pages, 2012.

[36] M. S. Hossain, A. K. Pandey, N. A. Rahim, J. Selvaraj, V. V. Tyagi, and M. M. Islam, "Self-cleaning assisted photovoltaic system with thermal energy storage: design and performance evaluation," *Solar Energy*, vol. 206, pp. 487–498, 2020.

[37] A. Ahmadi, M. A. Ehyaei, A. Doustgani et al., "Recent residential applications of low-temperature solar collector," *Journal of Cleaner Production*, vol. 279, article 123549, 2021.